

Michael Reichelt, BSc BSc

A Stable Finite Element Formulation for the Wave Equation in Space-Time

MASTER'S THESIS

to achieve the university degree of

Diplom-Ingenieur

Master's degree programme: Mathematics

submitted to

Graz University of Technology

Supervisor

Prof. Dr. O. Steinbach

Institute of Applied Mathematics

Graz, July 2022

Preface

This thesis gave me the opportunity to apply the knowledge acquired in my studies of Technomathematics at Graz University of Technology to an ongoing research topic, namely space time finite element methods for the wave equation. In this work different stabilization techniques are explored for the resulting numerical schemes. Unfortunately the goal of reaching an unconditionally stable formulation on unstructured grids could not be achieved. However on structured grids, the restrictions of the unstabilized version can be substantially relaxed.

Special thanks belong to Prof. Dr. Olaf Steinbach for the caring supervision and to my colleague Dipl.-Ing. Richard Löscher for always providing advice and assistance.

Contents

Abstract	7
Introduction	9
1 Preliminaries	11
1.1 Sobolev-Bochner Spaces	11
1.2 BBL Condition	12
1.3 Stability and Convergence of Multistep Methods	12
2 Wave Equation	15
2.1 Variational Formulation	15
2.2 Modified Time-Reversal Map	17
2.3 Semi-Discretization in Time	18
3 ODE Setting	21
4 Tensor Product Spaces	25
4.1 Projection onto Piecewise Constants in Time and Space	26
4.2 Projection onto Piecewise Constants in Time and Piecewise Linears in Space	28
4.3 Numerical Experiments	32
4.3.1 Notes on Implementation	32
4.3.2 Unstabilized Problem	35
4.3.3 Projection onto Piecewise Constants in Time and Space	36
4.3.4 Projection onto Piecewise Constants in Time and Piecewise Linears in Space	37
5 Regular Triangular Meshes	39
5.1 Numerical Experiments	40
5.1.1 No Stabilization	40
5.1.2 Projection onto Piecewise Linears	41
5.1.3 Projection onto Piecewise Linears with Mass Lumping	43
6 Conclusion and Outlook	45
Bibliography	47

Abstract

In this thesis the variational formulation of the wave equation in space-time and its finite element treatment are explored. As it turns out, the straightforward space-time variational formulation is not stable without restrictions on the mesh. To overcome this problem, stabilization techniques are introduced, which can completely remove the restrictions on tensor product ansatz spaces, substantially alleviate the restrictions on structured simplicial meshes but effective stabilizations for unstructured meshes are still an open problem.

Diese Arbeit beschäftigt sich mit Raum-Zeit-Formulierungen der Wellengleichung und deren Approximation mithilfe der Finite Elemente Methode. Es stellt sich heraus, dass das zugehörige Variationsproblem nicht ohne Restriktionen an die Vernetzung des Raum-Zeit-Bereiches stabil ist. Um dieses Problem zu überwinden, werden Stabilisierungstechniken eingeführt, die die Beschränkungen für Tensorprodukt-Ansatzräume vollständig aufheben und die Beschränkungen für strukturierte, simpliziale Netze erheblich verringern können. Jedoch sind effektive Stabilisierungen für unstrukturierte Netze immer noch ein offenes Problem.

Introduction

This work concentrates on finding a stabilization for the numerical solution of the wave equation in space-time. Traditionally, time dependent partial differential equations are either first discretized in space and subsequently in time or vice versa. For an introduction to these methods see e.g. [1]. In contrast to this approach finite element methods in space and time are investigated for the wave equation. This ultimately leads to 4-dimensional meshes, but in this paper the spatial dimension is set to one, leading to two-dimensional meshes. An extensive discussion on the solvability of the continuous variational formulation is given in [12]. Unfortunately the straightforward variational problem is not numerically stable without restrictions on the mesh, hence stabilization techniques are required. The ideas for stabilization date back to early work of Zlotnik [18], which are later picked up again and put into a more modern framework by Steinbach and Zank in [13]. They lead to unconditionally stable methods for tensor product ansatz spaces. The goal of this work is to extend this approach to simplicial meshes by reinterpreting the previous stabilizations as a coupled system. Unfortunately this cannot be achieved by the author, but it is possible to find stabilizations, which relax the restrictions on the mesh and additionally a new stabilization for tensor product meshes is found. There is also ongoing research on discontinuous Galerkin methods for parabolic and hyperbolic problems [4, 6], however these methods are outside of this work's scope.

This paper is structured as follows:

In Chapter 1 the necessary function spaces and characterizations for stability are introduced, followed by Chapter 2 which derives the continuous variational formulation for the wave equation in space-time. Inspired by a decomposition in spatial eigenfunctions of the Laplacian, Chapter 3 concentrates on the analysis and stabilization of the ordinary differential equations arising from this approach. Subsequently Chapter 4 extends these ideas to tensor product ansatz spaces and introduces a new stabilization for this setting, which is also unconditionally stable. Chapter 5 introduces stabilizations for triangular meshes. All numerical experiments are enabled by the excellent finite element framework MFEM [10].

1 Preliminaries

In this chapter the needed function spaces for the analysis of the wave equation and their properties are introduced. Further stability and convergence theory for multistep methods, which are introduced e.g. in [7, 15], is briefly recapitulated.

1.1 Sobolev-Bochner Spaces

Bochner spaces are a generalisation of the usual L^p spaces. For a more extensive introduction to this topic see [9].

Definition 1.1 (Bochner spaces). Let X be a separable Banach space with norm $\|\cdot\|$, $D \subset \mathbb{R}^n$ bounded and $p \in [0, \infty)$, then

$$L^p(D, X) = \{f : D \rightarrow X \mid f \text{ is Bochner measurable, } \|f\| \in L^p(D)\}.$$

In the case of time-dependent partial differential equations, we have $D = (0, T)$ with $T > 0$. In order to simplify notation, one sets

$$L^p(0, T; X) := L^p((0, T), X).$$

Analogous to classical Sobolev spaces, Sobolev-Bochner spaces are defined for the time-derivative:

Definition 1.2 (Sobolev-Bochner spaces). Let X be a separable Banach space with norm $\|\cdot\|$, then

$$H^1(0, T; X) = \{f \in L^2(0, T; X) \mid \partial_t f \in L^2(0, T; X)\},$$

where $\partial_t f$ is the weak temporal derivative of f . See [9, Chapter 3.2] for further information about weak derivatives on Bochner spaces.

On this space it is possible to impose initial and terminal conditions:

Definition 1.3.

$$\begin{aligned} H_0^1(0, T; X) &= \{u \in H^1(0, T; X) \mid u(0) = 0\}, \\ H_0^1(0, T; X) &= \{u \in H^1(0, T; X) \mid u(T) = 0\}. \end{aligned}$$

1.2 BBL Condition

The Babuška–Brezzi–Ladyzhenskaya (BBL) or generalized ellipticity condition is a useful tool to characterize the well-posedness of variational formulations. For a thorough introduction to this topic see [2].

Theorem 1.1 (BBL condition). *Let U, V be reflexive Banach spaces, $a : U \times V \rightarrow \mathbb{R}$ a bilinear form and $f \in V'$. Then the variational problem to find $u \in U$ such that*

$$a(u, v) = \langle f, v \rangle \quad \forall v \in V$$

is uniquely solvable if and only if the following conditions are met:

- *The bilinear form $a(\cdot, \cdot)$ is bounded, i.e.*

$$\exists c_B > 0 : |a(u, v)| \leq c_B \|u\|_U \|v\|_V \quad \forall u \in U, \forall v \in V.$$

- *The bilinear form obeys the inf-sup condition*

$$\exists c_S > 0 : \inf_{u \in U \setminus \{0\}} \sup_{v \in V \setminus \{0\}} \frac{a(u, v)}{\|u\|_U \|v\|_V} \geq c_S.$$

- *The associated operator $A : U \rightarrow V'$ is surjective, which is characterized by*

$$\forall v \in V \setminus \{0\} \exists u \in U : a(u, v) \neq 0.$$

Proof: See [2, Theorem 6.3].

1.3 Stability and Convergence of Multistep Methods

The arising finite element equation systems in this work can often be interpreted as linear multistep methods, which are known from the numerics of ordinary differential equations. For a general introduction to this topic see e.g. [7, 15]. However the main results on stability and convergence are revisited here. For this purpose consider the ordinary differential equation

$$\begin{aligned} y'(t) &= f(t, y) \quad \text{in } (0, T), \\ y(0) &= y_0, \end{aligned} \tag{1.1}$$

where f is a real valued function, $y_0 \in \mathbb{R}$ the initial condition and $T > 0$ a fixed time horizon. The unique solvability of this problem is assured by Picard's theorem:

Theorem 1.2 (Picard). *Let $T > 0$, $|f(t, y_0)| \leq K \forall t \in [0, T]$ and define the rectangular domain $D = [0, T] \times [y_0 - C, y_0 + C]$ for $C > 0$. Assume that f is continuous on D and that it further obeys the Lipschitz condition for a $L > 0$:*

$$|f(t, u) - f(t, v)| \leq L |u - v| \quad \forall (t, u), (t, v) \in D.$$

If it further holds true that

$$C \geq \frac{K}{L} (e^{LT} - 1),$$

then there exists an uniquely defined continuous solution y of problem (1.1).

Proof: See [15, Theorem 12.1]. □

For the numerical solution of problem (1.1) consider equally spaced points $t_k = kh$ for some mesh width $h > 0$ associated with corresponding function values y_k . A linear k -step method is given by the linear recurrence equation

$$\sum_{j=0}^k \alpha_j y_{n+j} = h \sum_{j=0}^k \beta_j f(t_{n+j}, y_{n+j})$$

and

$$\rho(z) = \sum_{j=0}^k \alpha_j z^j$$

is called its characteristic polynomial. Note that a k -step method requires k starting values, which have to be computed by other means. Zero-stability ensures that the solution of a multistep method for a fixed maximal time horizon T stays bounded as $h \rightarrow 0$ and can be formally defined by:

Definition 1.4 (zero-stability). A linear multistep method is zero-stable if there exists $K > 0$ such that for two different sets of starting values y_0, \dots, y_{k-1} and u_0, \dots, u_{k-1} and a fixed maximal time horizon T , the generated solution sequences $(y_n)_n$, $(u_n)_n$ obey

$$|y_n - u_n| \leq K \max_{i=0, \dots, k-1} \{|y_i - u_i|\}$$

as $h \rightarrow 0$.

A direct verification of zero-stability is tedious. The following theorem gives an algebraic characterization of that property, which is easy to examine for any multistep method:

Theorem 1.3 (Root condition). *A linear multistep method is zero-stable if and only if all the roots of its characteristic polynomial are inside the closed complex unit disc and all roots with absolute value of one are simple.*

Proof: See [15, Theorem 12.4]. □

Note that there is no dependency on the right hand side f in the root condition, hence the name zero-stability is justified. To investigate convergence one additionally defines consistency and order of accuracy of the method:

Definition 1.5. A linear k -step method is said to be **consistent** if $\forall \varepsilon > 0$ there exists an $h(\varepsilon) > 0$ such that

$$|T_n(h)| < \varepsilon \quad \text{for } 0 < h < h(\varepsilon),$$

on any (continuous) solution curve of problem (1.1) on D as in Picard's theorem, where

$$T_n := \frac{\sum_{j=0}^k [\alpha_j y(t_{n+j}) - h \beta_j f(t_{n+j}, y(t_{n+j}))]}{h \sum_{j=0}^k \beta_j}$$

is called truncation error. Further the multistep method is said to have **order of accuracy** $p \in \mathbb{N}$ if there exists $K > 0$ such that

$$|T_n(h)| \leq K h^p \quad \text{for } 0 < h < h(\varepsilon).$$

With all these prerequisites the main theorem about convergence of multistep methods can be stated:

Theorem 1.4 (Dahlquist's equivalence). *Consider a **consistent** linear k -step method for the ordinary differential equation (1.1) with all assumptions of Picard's theorem fulfilled for a fixed time horizon T . Further let y_0, \dots, y_{k-1} be consistent starting values, i.e.*

$$y_i \rightarrow y_0 \quad \text{as } h \rightarrow 0 \quad \text{for } i = 0, \dots, k-1.$$

Then this k -step method is convergent if and only if it is zero-stable. Furthermore if the method is of order of accuracy p and the solution y has continuous derivatives up to order $p+1$, then there holds the error estimate

$$|y(x_n) - y_n| \leq K h^p$$

for some constant $K > 0$ as $h \rightarrow 0$.

Proof: See [5, Theorem 6.3.4] or the references in [15, Theorem 12.5]. □

2 Wave Equation

In this work, the wave equation with homogeneous boundary and initial conditions is considered. Let $\Omega \subset \mathbb{R}^n$ be a bounded Lipschitz domain with boundary $\partial\Omega$, then the wave equation in strong form reads as

$$\begin{aligned} \partial_{tt}u(t, x) - \Delta_x u(t, x) &= f(t, x) && \text{for } (t, x) \in Q := (0, T) \times \Omega, \\ u(t, x) &= u(t, x) = 0 && \text{for } (t, x) \in \Sigma := (0, T) \times \partial\Omega, \\ u(0, x) &= \partial_t u(t, x)|_{t=0} = 0 && \text{for } x \in \Omega. \end{aligned} \quad (2.1)$$

In this setting Q is called the space-time-cylinder and Σ is its lateral boundary. Following previous work in [13] and [14] a variational formulation of (2.1) is deduced and its appropriate function spaces are introduced.

2.1 Variational Formulation

To obtain a variational formulation, the wave equation is multiplied with a test function v , sufficiently smooth for all operations to be well defined:

$$\partial_{tt}u(t, x)v(t, x) - \Delta_x u(t, x)v(t, x) = f(t, x)v(t, x)$$

Integration and integration by parts in space yields

$$\begin{aligned} \int_{\Omega} \partial_{tt}u(t, x)v(t, x)dx + \int_{\Omega} \nabla_x u(t, x) \cdot \nabla_x v(t, x)dx - \int_{\partial\Omega} v(t, x) \nabla_x u(t, x) \cdot n_x ds_x \\ = \int_{\Omega} f(t, x)v(t, x)dx, \end{aligned}$$

where n_x is the outward unit normal vector on $\partial\Omega$. With regards to the boundary conditions claiming $u(t, \cdot)|_{\partial\Omega} = v(t, \cdot)|_{\partial\Omega} = 0$ is reasonable, yielding

$$\int_{\Omega} \partial_{tt}u(t, x)v(t, x)dx + \int_{\Omega} \nabla_x u(t, x) \cdot \nabla_x v(t, x)dx = \int_{\Omega} f(t, x)v(t, x)dx.$$

Integration and integration by parts in time gives

$$\begin{aligned} - \int_Q \partial_t u(t, x) \partial_t v(t, x) dx dt + \int_\Omega [\partial_t u(t, x) v(t, x)]_0^T dx + \int_Q \nabla_x u(t, x) \cdot \nabla_x v(t, x) dx dt \\ = \int_Q f(t, x) v(t, x) dx dt. \end{aligned}$$

By claiming $v(T, x) = 0$ and noting $\partial_t u(t, x)|_{t=0} = 0$ the spatial integral vanishes and one obtains the weak form

$$- \int_Q \partial_t u(t, x) \partial_t v(t, x) dx dt + \int_Q \nabla_x u(t, x) \cdot \nabla_x v(t, x) dx dt = \int_Q f(t, x) v(t, x) dx dt.$$

The appropriate function spaces are $H_{0;0}^{1,1}(Q)$ for u and $H_{0;0}^{1,1}(Q)$ for v , where

$$\begin{aligned} H_{0;0}^{1,1}(Q) &= L^2(0, T; H_0^1(\Omega)) \cap H_0^1(0, T; L^2(\Omega)), \\ H_{0;0}^{1,1}(Q) &= L^2(0, T; H_0^1(\Omega)) \cap H_0^1(0, T; L^2(\Omega)). \end{aligned}$$

An appropriate norm on these spaces is

$$\|u\|_{H_{0;0}^{1,1}(Q)} = \sqrt{\|u\|_{L^2(0,T;H_0^1(\Omega))}^2 + \|\partial_t u\|_{L^2(Q)}^2},$$

where

$$\|u\|_{L^2(0,T;H_0^1(\Omega))}^2 = \int_0^T \int_\Omega |\nabla_x u(t, x)|^2 dx dt.$$

Remark 2.1. The norm $\|\cdot\|_{H_{0;0}^{1,1}(Q)}$ is induced by the scalar product

$$(u, v)_{H_{0;0}^{1,1}(Q)} = \int_Q (\nabla_x u(t, x) \cdot \nabla_x v(t, x) + \partial_t u(t, x) \partial_t v(t, x)) dx dt.$$

$H_{0;0}^{1,1}(Q)$ as well as $H_{0;0}^{1,1}(Q)$ are Hilbert spaces with respect to this norm. For further details see [9] or [17].

Theorem 2.1. *The variational problem for the wave equation to find $u \in H_{0;0}^{1,1}(Q)$ such that*

$$a(u, v) = \langle f, v \rangle_{L^2(Q)} \quad \forall v \in H_{0;0}^{1,1}(Q) \quad (2.2)$$

is uniquely solvable for $f \in L^2(Q)$, where

$$a(u, v) = - \int_Q \partial_t u(t, x) \partial_t v(t, x) dx dt + \int_Q \nabla_x u(t, x) \cdot \nabla_x v(t, x) dx dt.$$

The solution u obeys the stability estimate

$$\|u\|_{H_{0;0}^{1,1}(Q)} \leq \frac{T}{\sqrt{2}} \|f\|_{L^2(Q)}.$$

Proof: See [14, Theorem 5.1]. □

Remark 2.2. Note that the variational formulation (2.2) uses different ansatz and test spaces and is therefore of Petrov-Galerkin type.

2.2 Modified Time-Reversal Map

To mitigate the problem of different ansatz and test spaces it is convenient to define a modified time-reversal map, as introduced in [17].

Definition 2.1 (Modified Time-Reversal Map).

$$\begin{aligned} T_R &: H_{0;0}^{1,1}(Q) \rightarrow H_{0;0}^{1,1}(Q) \\ (T_R u)(t, x) &= u(T, x) - u(t, x) \end{aligned}$$

Lemma 2.2. The modified time-reversal map is an isomorphism and its inverse is given by

$$(T_R^{-1} v)(t, x) = v(0, x) - v(t, x).$$

Proof:

- T_R and T_R^{-1} are obviously bounded.
- To show that T_R is bijective directly verify the inverse

$$\begin{aligned} (T_R^{-1} T_R u)(t, x) &= (T_R u)(0, x) - (T_R u)(t, x) \\ &= u(T, x) - \underbrace{u(0, x)}_{=0} - u(T, x) + u(t, x) = u(t, x) \text{ a.e.} \\ (T_R T_R^{-1} v)(t, x) &= (T_R^{-1} v)(T, x) - (T_R^{-1} v)(t, x) \\ &= v(0, x) - \underbrace{v(T, x)}_{=0} - v(0, x) + v(t, x) = v(t, x) \text{ a.e.} \end{aligned}$$

□

The modified time-reversal map admits an equivalent variational formulation to (2.2) with the same ansatz and test space, to find $u \in H_{0;0}^{1,1}(Q)$ such that

$$a(u, T_R v) = \langle f, T_R v \rangle_{L^2(Q)} \quad \forall v \in H_{0;0}^{1,1}(Q), \quad (2.3)$$

again for $f \in L^2(Q)$.

Further it yields a convenient property for the term involving the time derivatives, as stated in the following corollary.

Corollary 2.3. $\forall u, v \in H_{0;0}^{1,1}(Q)$ it obviously holds true, that

$$-\langle \partial_t u, \partial_t T_R v \rangle_{L^2(Q)} = \langle \partial_t u, \partial_t v \rangle_{L^2(Q)}.$$

A naive idea is to directly apply continuous Galerkin methods to variational problem (2.3) using e.g. piecewise linear ansatz functions on a simplicial mesh. However it turns out, that in this case a CFL-condition is needed, which is detrimental for e.g. adaptivity. More elaborations on that topic as well as numerical experiments are presented in Chapters 4.3.2 and 5.1.1 for a quadrilateral and a triangular grid.

2.3 Semi-Discretization in Time

For the analysis of the wave equation - especially on tensor product ansatz spaces - it proves useful to consider a semi-discretization approach following [14]. For this purpose remember that the eigenfunctions of the Laplacian $(\psi_n)_{n=1}^\infty$ fulfilling

$$\begin{aligned} -\Delta_x \psi_n &= \lambda_n \psi_n & \text{in } \Omega \\ \psi_n &= 0 & \text{on } \partial\Omega \end{aligned}$$

with $0 < \lambda_1 \leq \lambda_2 \leq \dots$ form an orthonormal basis in $L^2(\Omega)$ and a basis in $H_0^1(\Omega)$ (see e.g. [1]). This means that every $u \in L^2(0, T; H_0^1(\Omega))$ has the representation

$$\begin{aligned} u(t, x) &= \sum_{i=1}^{\infty} U_i(t) \psi_i(x), \\ U_i(t) &= \int_{\Omega} u(t, x) \psi_i(x) dx. \end{aligned}$$

Substituting this representation in the variational formulation (2.2) using the test function

$$v(t, x) = V_j(t) \psi_j(x) \quad (2.4)$$

yields

$$\begin{aligned}
a(u, v) &= \sum_{i=1}^{\infty} a(U_i \psi_i, V_j \psi_j) \\
&= \sum_{i=1}^{\infty} \left\{ \int_0^T \partial_t U_i(t) \partial V_j(t) dt \int_{\Omega} \psi_i(x) \psi_j(x) dx \right. \\
&\quad \left. + \int_0^T U_i(t) V_j(t) dt \int_{\Omega} \nabla_x \psi_i(x) \nabla_x \psi_j(x) dx \right\} \\
&= \sum_{i=1}^{\infty} \left\{ \int_0^T \partial_t U_i(t) \partial V_j(t) dt \delta_{i,j} + \int_0^T U_i(t) V_j(t) dt \lambda_i \delta_{i,j} \right\} \\
&= \int_0^T \partial_t U_j(t) \partial V_j(t) dt + \lambda_j \int_0^T U_j(t) V_j(t) dt = \int_0^T V_j(t) \underbrace{\int_{\Omega} f(t, x) \psi_j(x) dx}_{=f_j(t)} dt,
\end{aligned}$$

where $\delta_{i,j}$ is the Kronecker delta. Further the orthogonality and the eigenvalue problem of the ψ_i are used. Since test functions of the form (2.4) are a basis of the test space the variational formulation can be considered separately for every eigenfunction of the Laplacian as a variational problem to find $U_i \in H_{0,}^1(0, T)$ such that

$$\int_0^T \partial_t U_i(t) \partial V_j(t) dt + \lambda_i \int_0^T U_i(t) V_j(t) dt = \int_0^T f_i(t) V_j(t) dt \quad \forall V_j \in H_{0,}^1(0, T), \quad (2.5)$$

which is the weak form of

$$\begin{aligned}
\partial_{tt} U_i(t) + \lambda_i U_i(t) &= f_i(t) \quad \text{for } t \in (0, T), \\
U_i(0) &= U_i'(0) = 0.
\end{aligned}$$

3 ODE Setting

Motivated by the semi-discretization approach presented in the previous chapter, this chapter investigates the ordinary differential equation (ODE)

$$\begin{aligned}\partial_{tt}u(t) + \mu u(t) &= f(t) \quad \text{for } t \in (0, T), \\ u(0) &= u'(0) = 0,\end{aligned}$$

where $f \in L^2(0, T)$, $\mu > 0$ and $T > 0$. This chapter follows [13] closely, but interprets the presented stabilization differently to allow for a generalization to simplicial meshes. The associated weak formulation derived analogously to (2.5) is to find $u \in H_0^1(0, T)$ such that

$$-\int_0^T \partial_t u(t) \partial_t v(t) dt + \mu \int_0^T u(t) v(t) dt = \int_0^T f(t) v(t) dt \quad \forall v \in H_0^1(0, T). \quad (3.1)$$

Let $\mathcal{T}_h = \{\tau_n\}_{n=1}^{N_h}$ be a uniform decomposition of $(0, T)$ into intervals τ_n with

$$\text{diam } \tau_n = h.$$

When applying a Galerkin-Petrov discretization to (3.1) using the ansatz and test spaces

$$\begin{aligned}U_h &= P^1(\mathcal{T}_h) \cap H_0^1(0, T), \\ V_h &= P^1(\mathcal{T}_h) \cap H_{,0}^1(0, T),\end{aligned}$$

where $P^1(\mathcal{T}_h)$ are the piecewise linear functions on \mathcal{T}_h , it turns out (see [13, page 345]), that the associated formulation to find $u_h \in U_h$ such that

$$-\int_0^T \partial_t u_h(t) \partial_t v_h(t) dt + \mu \int_0^T u_h(t) v_h(t) dt = \int_0^T f(t) v_h(t) dt \quad \forall v_h \in V_h \quad (3.2)$$

is stable for

$$h < \sqrt{\frac{12}{\mu}}.$$

The proof for this statement is revisited in the following lemma:

Lemma 3.1. *The variational problem (3.2) discretized on an uniform mesh with mesh width h is stable for*

$$h < \sqrt{\frac{12}{\mu}}.$$

Proof: The variational formulation (3.2) using nodal piecewise linear ansatz functions ψ_i corresponds to the equation system

$$\left\{ \frac{1}{h} \begin{pmatrix} 1 & & & & \\ & -2 & & & \\ & & \ddots & & \\ & 1 & & \ddots & \\ & & & & 1 & -2 & 1 \end{pmatrix} + \frac{\mu h}{6} \begin{pmatrix} 1 & & & & \\ & 4 & & & \\ & & \ddots & & \\ & 1 & & \ddots & \\ & & & & 1 & 4 & 1 \end{pmatrix} \right\} \begin{pmatrix} u_1 \\ u_2 \\ \vdots \\ u_n \end{pmatrix} = \begin{pmatrix} f_0 \\ f_1 \\ \vdots \\ f_{n-1} \end{pmatrix}, \quad (3.3)$$

where

$$f_i = \int_0^T f(t) \psi_i(t) dt$$

and the initial and terminal conditions of the ansatz and test space are included through elimination of columns and rows. The matrix system (3.3) can be interpreted as a two-step method

$$(6 + \mu h^2) u_{k+2} + (4\mu h^2 - 12) u_{k+1} + (6 + \mu h^2) u_k = 6h f_{k+1}.$$

Note that u_0 is given by the initial condition and u_1 can be directly calculated from the first matrix line. The characteristic polynomial of this two-step method is

$$\rho(z) = (6 + \mu h^2) z^2 + (4\mu h^2 - 12) z + (6 + \mu h^2).$$

Its roots are given by

$$z_{1,2} = \frac{1}{6 + \gamma} \left(6 - 2\gamma \pm \sqrt{3\gamma(\gamma - 12)} \right),$$

where

$$\gamma = \mu h^2.$$

To fulfil the root condition (Theorem 1.3) all roots must be of absolute value less or equal to one. Further if a root is of absolute value one, it must be simple. Analyzing the different cases:

- $\gamma = 12$

In this case there is a double root so it must hold true that

$$\left| \frac{6 - 2\gamma}{6 + \gamma} \right| = \frac{18}{18} < 1,$$

which is obviously not fulfilled.

- $\gamma > 12$

For the second root the necessary condition

$$\frac{1}{6 + \gamma} \left(6 - 2\gamma - \sqrt{3\gamma(\gamma - 12)} \right) \geq -1$$

is violated as reorganization of terms shows:

$$0 \underbrace{\leq}_{\gamma > 12} \sqrt{3\gamma(\gamma - 12)} \leq 12 - \gamma \underbrace{\leq}_{\gamma > 12} 0.$$

- $\gamma < 12$

In this case the roots are simple and complex

$$z_{1,2} = \frac{1}{6 + \gamma} \left(6 - 2\gamma \pm i\sqrt{36\gamma - 3\gamma^2} \right)$$

with absolute value

$$|z_{1,2}| = \frac{6^2 + 12\gamma + \gamma^2}{(6 + \gamma)^2} = 1,$$

hence the root condition is fulfilled.

So the system is only stable for

$$12 > \gamma = \mu h^2$$

yielding the claimed CFL condition. \square

To overcome the restriction on the mesh size the authors of [13] introduce the L^2 -Projection Q_h^0 onto piecewise constants $P^0(\mathcal{T}_h)$, defined for $u_h \in P^1(\mathcal{T}_h)$ by

$$\langle Q_h^0 u_h, q_h \rangle_{L^2(0,T)} = \langle u_h, q_h \rangle_{L^2(0,T)} \quad \forall q_h \in P^0(\mathcal{T}_h)$$

and introduce the stabilized variational problem to find $u_h \in U_h$ such that

$$\tilde{a}_h(u_h, v_h) := -\langle \partial_t u_h, \partial_t v_h \rangle_{L^2(0,T)} + \mu \langle Q_h^0 u_h, v_h \rangle_{L^2(0,T)} = \langle f, v_h \rangle_{(0,T)} \quad \forall v_h \in V_h \quad (3.4)$$

which is unconditionally stable, as stated in the following theorem.

Theorem 3.2. *Let $\mathcal{T}_h = \{\tau_n\}_{n=1}^{N_h}$ be a decomposition of $(0, T)$ into intervals τ_n with maximal mesh size h , then the variational problem to find $u_h \in U_h$ such that*

$$\tilde{a}_h(u_h, v_h) := -\langle \partial_t u_h, \partial_t v_h \rangle_{L^2(0,T)} + \mu \langle Q_h^0 u_h, v_h \rangle_{L^2(0,T)} = \langle f, v_h \rangle_{(0,T)} \quad \forall v_h \in V_h$$

is uniquely solvable independent of the mesh size h and admits the stability estimate for each $u_h \in U_h$

$$\frac{1}{1 + \sqrt{2}\mu T} |u_h|_{H^1(0,T)} \leq \sup_{0 \neq v_h \in V_h} \frac{\tilde{a}_h(u_h, v_h)}{|v_h|_{H^1(0,T)}}.$$

Further the approximation error can be bounded for a solution $u \in H^s(0, T)$ with $s \in [1, 2]$ by

$$\begin{aligned} |u - u_h|_{H^1(0,T)} \leq & \left[1 + \left(1 + \frac{1}{2}\mu T^2 \right) \left(1 + \sqrt{2}\mu T^2 \right) \right] C_1(s) h^{s-1} |u|_{H^s(0,T)} \\ & + \frac{1}{12}\mu \left(1 + \sqrt{2}\mu T^2 \right) h^2 C_s |u|_{H^1(0,T)} \end{aligned}$$

with $C_1, C_2 > 0$ and the standard Sobolev seminorms $|\cdot|_{H^s(0,T)}$.

Proof: See [13, Lemma 17.6 and Theorem 17.1]. □

The variational problem (3.4) can be realized without explicit use of the projection onto piecewise constants Q_h^0 as a system to find $u_h \in U_h, p_h \in P_h$ such that

$$\begin{aligned} -\langle \partial_t u_h, \partial_t v_h \rangle_{L^2(0,T)} + \mu \langle p_h, v_h \rangle_{L^2(0,T)} &= \langle f, v_h \rangle_{(0,T)} \\ -\langle p_h, q_h \rangle_{L^2(0,T)} + \langle u_h, q_h \rangle_{L^2(0,T)} &= 0 \quad \forall v_h \in V_h, \forall q_h \in P_h \end{aligned} \quad (3.5)$$

where the space $P_h = P^0(\mathcal{T}_h)$. Note that the second equation of (3.5) is the definition of $Q_h^0 u_h = p_h$.

4 Tensor Product Spaces

This chapter extends on the ideas of the semi-discretization approach and the considerations on stability for the ODE setting. For ease of presentation $\Omega = (0, 1)$, but most of the results can be extended to higher spatial dimensions (see [13]). The variational problem of interest is to find $u_h \in U_h, p_h \in P_h$ such that

$$\begin{aligned} -\langle \partial_t u_h, \partial_t v_h \rangle_{L^2(Q)} + \langle p_h, \partial_x v_h \rangle_{L^2(Q)} &= \langle f, v_h \rangle_Q \\ \langle \partial_x u_h, q_h \rangle_{L^2(Q)} - \langle p_h, q_h \rangle_{L^2(Q)} &= 0 \quad \forall v_h \in V_h, q_h \in P_h. \end{aligned} \quad (4.1)$$

For ansatz and test spaces, tensor products of space and time ansatz spaces are considered. Let $X_h \subset H_0^1(\Omega)$, $T_{h,0} \subset H_0^1(0, T)$, $T_{h,0} \subset H_{,0}^1(0, T)$, $\tilde{X}_h \subset L^2(\Omega)$ and $\tilde{T}_h \subset L^2(0, T)$ be conforming finite dimensional ansatz spaces. Then

$$\begin{aligned} U_h &= T_{h,0} \otimes X_h \\ V_h &= T_{h,0} \otimes X_h \\ P_h &= \tilde{T}_h \otimes \tilde{X}_h. \end{aligned}$$

In the following sections two specific choices for the spaces are considered. One is a reinterpretation of [13] as a system and the other differs in the choice of \tilde{X}_h . Nevertheless both turn out to be stable, without restrictions on the used meshes in space and time.

Remark 4.1. For finite dimensional real function spaces $T = \text{span}\{\psi_i(\cdot)\}_{i=1}^{N_t}$ and $X = \text{span}\{\varphi_k(\cdot)\}_{k=1}^{N_x}$, a function $u \in T \otimes X$ by construction has the representation

$$u(t, x) = \sum_{i=1}^{N_t} \sum_{k=1}^{N_x} \alpha_{i,k} \psi_i(t) \varphi_k(x) = \sum_{k=1}^{N_x} T_k(t) \varphi_k(x) = \sum_{i=1}^{N_t} X_i(x) \psi_i(t),$$

where $\alpha_{i,k} \in \mathbb{R}$ and

$$\begin{aligned} T_k(t) &= \sum_{i=1}^{N_t} \alpha_{i,k} \psi_i(t), \\ X_i(x) &= \sum_{k=1}^{N_x} \alpha_{i,k} \varphi_k(x). \end{aligned}$$

4.1 Projection onto Piecewise Constants in Time and Space

In this section the aforementioned reinterpretation of [13] as a system for the ODE setting is further investigated in the setting of the one-dimensional wave equation. For this purpose let $\mathcal{T}_h = \{\tau_n\}_{n=1}^{N_t}$ and $\mathcal{X}_h = \{\chi_n\}_{n=1}^{N_x}$ be decompositions of $(0, T)$ and $(0, 1)$ into intervals. For U_h and V_h piecewise linear functions in space and time are used, whereas for P_h piecewise constants in space and time are used, i.e.

$$\begin{aligned} X_h &= P^1(\mathcal{X}_h) \cap H_0^1(0, 1) \\ T_{h;0} &= P^1(\mathcal{T}_h) \cap H_{0,0}^1(0, T) \\ T_{h;,\infty} &= P^1(\mathcal{T}_h) \cap H_{,\infty}^1(0, T) \\ \tilde{X}_h &= P^0(\mathcal{X}_h) \\ \tilde{T}_h &= P^0(\mathcal{T}_h). \end{aligned} \quad (4.2)$$

As the following lemma shows, this is equivalent to the stabilization introduced in [13] to find $u_h \in U_h$ such that

$$-\langle \partial_t u_h, \partial_t v_h \rangle_{L^2(Q)} + \langle Q_{h,t}^0 \partial_x u, \partial_x v \rangle_{L^2(Q)} = \langle f, v_h \rangle_Q \quad \forall v_h \in V_h, \quad (4.3)$$

where $Q_{h,t}^0 : L^2(0, T) \rightarrow P^0(\mathcal{T}_h) = \tilde{T}_h$ is the projection onto constants in time defined by

$$\langle Q_{h,t}^0 w, \tilde{\psi}_h \rangle_{L^2(0,T)} = \langle w, \tilde{\psi}_h \rangle_{L^2(0,T)} \quad \forall \tilde{\psi}_h \in \tilde{T}_h.$$

Remark 4.2. For tensor product spaces the projection onto constants in time $Q_{h,t}^0$ obviously only acts on the temporal part of the function. So actually $Q_{h,t}^0$ has to be considered as

$$Q_{h,t}^0 \otimes I_x,$$

where I_x is the identity in the context dependent spatial function space. To see this consider Remark 4.1. But for the sake of easier notation, this detail is mostly omitted.

Lemma 4.1. *The variational problem (4.1) and (4.3) are equivalent when we consider function spaces (4.2).*

Proof: Consider the representation as in Remark 4.1

$$\begin{aligned} p_h(t, x) &= \sum_{j=1}^{\dim \tilde{T}_h} \sum_{l=1}^{\dim \tilde{X}_h} p_{j,l} \tilde{\psi}_j(t) \tilde{\varphi}_l(x) & p_{j,l} &\in \mathbb{R}, \\ u_h(t, x) &= \sum_{i=1}^{\dim T_{h;0}} \sum_{k=1}^{\dim X_h} u_{i,k} \psi_i(t) \varphi_k(x) & u_{i,k} &\in \mathbb{R}, \end{aligned}$$

where $\tilde{\psi}_j$ are the piecewise constants in time and $\tilde{\varphi}_l$ are the piecewise constants in space and ψ_i, φ_k the respective piecewise linear basis functions. Using this representation in the second equation of (4.1) yields

$$\sum_{j=1}^{\dim \tilde{T}_h} \sum_{l=1}^{\dim \tilde{X}_h} p_{j,l} \langle \tilde{\psi}_j, \tilde{\psi}_m \rangle_{L^2(0,T)} \langle \tilde{\varphi}_l, \tilde{\varphi}_s \rangle_{L^2(0,1)} = \sum_{i=1}^{\dim T_{h;0}} \sum_{k=1}^{\dim X_h} u_{i,k} \langle \psi_i, \tilde{\psi}_m \rangle_{L^2(0,T)} \langle \partial_x \varphi_k, \tilde{\varphi}_s \rangle_{L^2(0,1)} \quad \forall \tilde{\psi}_m \in \tilde{T}_h, \forall \tilde{\varphi}_s \in \tilde{X}_h.$$

This equation is uniquely solvable since the left hand side corresponds (given an appropriate ordering of indices) to the matrix $M_t^0 \otimes M_x^0$, where M_t^0 and M_x^0 are the mass-matrices for piecewise constant ansatz functions. It is well known that these matrices are positive definite, see e.g. [11]. Since $\partial_x \varphi_k \in \tilde{X}_h$, it has a representation in \tilde{X}_h yielding

$$\sum_{j=1}^{\dim \tilde{T}_h} \sum_{l=1}^{\dim \tilde{X}_h} p_{j,l} \langle \tilde{\psi}_j, \tilde{\psi}_m \rangle_{L^2(0,T)} \langle \tilde{\varphi}_l, \tilde{\varphi}_s \rangle_{L^2(0,1)} = \sum_{i=1}^{\dim T_{h;0}} \sum_{l=1}^{\dim \tilde{X}_h} \tilde{u}_{i,l} \langle \psi_i, \tilde{\psi}_m \rangle_{L^2(0,T)} \langle \tilde{\varphi}_l, \tilde{\varphi}_s \rangle_{L^2(0,1)} \quad \forall \tilde{\psi}_m \in \tilde{T}_h, \forall \tilde{\varphi}_s \in \tilde{X}_h.$$

Using the fact that $\langle \tilde{\varphi}_l, \tilde{\varphi}_s \rangle_{L^2(0,1)} = h_l^x \delta_{l,s}$, where $h_s^x = \text{diam } \chi_s$, the spatial sum vanishes on both sides

$$\sum_{j=1}^{\dim \tilde{T}_h} p_{j,s} \langle \tilde{\psi}_j, \tilde{\psi}_m \rangle_{L^2(0,T)} h_s^x = \sum_{i=1}^{\dim T_{h;0}} \tilde{u}_{i,s} \langle \psi_i, \tilde{\psi}_m \rangle_{L^2(0,T)} h_s^x \quad \forall \tilde{\psi}_m \in \tilde{T}_h, \forall s \in \{1, 2, \dots, \dim \tilde{X}_h\}.$$

So for every spatial basis function the projection onto constants in time remains, meaning

$$p_h = (Q_{h,t}^0 \otimes I_{0,x}) \partial_x u_h \in \tilde{T}_h \otimes \tilde{X}_h$$

where $I_{0,x}$ is the identity on $P^0(\mathcal{X}) = \tilde{X}_h$, which concludes the proof. \square

Now that both problems are shown to be equivalent, the following theorem investigates its unique solvability.

Theorem 4.2. *The variational problem (4.3) (and hence also (4.1)) is uniquely solvable for the function space choices (4.2). And the solution u_h obeys the stability estimate*

$$\|u_h\|_{L^2(Q)} \leq 2T \|f\|_{[H_{,0}^1(0,T;L^2(\Omega))]'}$$

and the error estimate (provided a sufficiently smooth solution u)

$$\begin{aligned} \|u - u_h\|_{L^2(Q)} &\leq ch_x^2 \left(\|u\|_{L^2(0,T;H^2(\Omega))} + \|\partial_t u\|_{L^2(0,T;H^2(\Omega))} \right) + \\ &\quad ch_x h_t \|\partial_t \nabla_x u\|_{L^2(Q)} + ch_t^2 \left(\|\partial_{tt} u\|_{L^2(Q)} + \|\partial_{tt} \Delta_x u\|_{L^2(Q)} \|\partial_t \Delta_x u\|_{L^2(Q)} \right), \end{aligned}$$

where h_t is the temporal, h_x the spatial mesh width.

Proof: see [13, page 362 et sqq.].

Remark 4.3. The natural choice when looking at derivatives would be $\tilde{T}_h = P^1(\mathcal{T}_h)$ since the spatial derivative only reduces the polynomial degree in space by 1. But evidently this leads to the original variational formulation without stabilization, which must fulfill the CFL-condition

$$h_t \leq \frac{1}{\sqrt{c_I}} h_x, \quad (4.4)$$

where h_t is the temporal, h_x the spatial mesh width and $c_I > 0$ is a constant stemming from an inverse inequality (see [14, page 192]).

Remark 4.4. The tensor product approach is equivalent to choosing piecewise bilinear ansatzfunctions for u_h and piecewise constant ansatz functions for p_h on an uniform quadrilateral mesh. This holds true by construction of the ansatz functions on quadrilaterals.

4.2 Projection onto Piecewise Constants in Time and Piecewise Linears in Space

In this section a slightly different approach as done in the previous chapter is introduced. Instead of piecewise constant functions for \tilde{X}_h , piecewise linear functions are used. So variational problem (4.1) with the function spaces

$$\begin{aligned} X_h &= P^1(\mathcal{X}_h) \cap H_0^1(0, 1) \\ T_{h;0} &= P^1(\mathcal{T}_h) \cap H_{0,0}^1(0, T) \\ T_{h;0} &= P^1(\mathcal{T}_h) \cap H_{,0}^1(0, T) \\ \tilde{X}_h &= P^1(\mathcal{X}_h) \cap H^1(\Omega) \\ \tilde{T}_h &= P^0(\mathcal{T}_h). \end{aligned} \quad (4.5)$$

is considered. An analogous analysis as in the previous chapter yields

$$p_h = (Q_{h,t}^0 \otimes Q_{h,x}^1) \partial_x u_h,$$

where $Q_{h,x}^1 : L^2(0,1) \rightarrow P^1(\mathcal{X}_h) = \tilde{X}_h$ is the projection onto piecewise linear functions, defined by

$$\langle Q_{h,x}^1 v, \tilde{\varphi}_h \rangle_{L^2(0,1)} = \langle v, \tilde{\varphi}_h \rangle_{L^2(0,1)} \quad \forall \tilde{\varphi}_h \in \tilde{X}_h = P^1(\mathcal{X}_h).$$

It turns out, that this problem is also unconditionally stable for periodic spatial boundary conditions, i.e.

$$u(t, 0) = u(t, 1)$$

as the following theorem states. This restriction is made out of technical reasons in the proof. However numerical experiments imply, that this is also the case for homogeneous boundary conditions.

Theorem 4.3. *The variational problem (4.1) for function spaces (4.5) with the restriction to periodic boundary conditions and uniform mesh size h_x in space and h_t in time is unconditionally stable.*

Proof: *To prove stability of the system a von Neumann stability analysis is conducted. For a general introduction to this topic see [8]. The core idea of the von Neumann analysis is to represent the spatial part of u_h and p_h by discrete Fourier modes. Out of this reason one has to consider periodic spatial boundary conditions. Since the resulting equation system is linear, stability can be examined for every Fourier mode separately, i.e.*

$$\begin{aligned} u_h &\rightarrow U^n e^{im\pi h_x} \\ p_h &\rightarrow P^n e^{im\pi h_x}, \end{aligned}$$

where U^n, P^n are the coefficients of the modes at time step n . Note that Fourier modes are eigenvectors of every difference operator and orthogonal under summation, hence only one spatial mode has to be considered at a time. For a more thorough introduction to discrete Fourier modes and difference operators see the discussion on local Fourier analysis in [16]. After a correct ordering of indices the resulting system of (4.1) can be represented as

$$(K_t \otimes M_x^1) \vec{u}_h + (M_t^{0,1} \otimes G_x^T) \vec{p}_h = 0 \quad (4.6)$$

$$(M_t^0 \otimes M_x^1) \vec{p}_h = (M_t^{1,0} \otimes G_x) \vec{u}_h \quad (4.7)$$

Note that the von Neumann stability analysis is closely related to zero-stability, hence set $f = 0$. The resulting finite element matrices are

$$\begin{aligned}
 K_t &= \frac{1}{h_t} \begin{pmatrix} 2 & -1 & & -1 \\ -1 & 2 & -1 & \\ & \ddots & \ddots & \ddots \\ & & -1 & 2 \\ -1 & & & -1 & 2 \end{pmatrix} \\
 M_x^1 &= \frac{h_x}{6} \begin{pmatrix} 4 & 1 & & 1 \\ 1 & 4 & 1 & \\ & \ddots & \ddots & \ddots \\ & & 1 & 4 \\ 1 & & & 1 & 4 \end{pmatrix} \\
 M_t^{0,1} &= \frac{h_t}{2} \begin{pmatrix} 1 & & & \\ 1 & 1 & & \\ & \ddots & \ddots & \ddots \\ & & 1 & 1 \end{pmatrix} \\
 M_t^{1,0} &= \frac{h_t}{2} \begin{pmatrix} 1 & 1 & & \\ & 1 & 1 & \\ & & \ddots & \ddots \\ & & & 1 & 1 \end{pmatrix} \\
 M_t^0 &= h_t \begin{pmatrix} 1 & & & \\ & 1 & & \\ & & \ddots & \ddots \\ & & & 1 \end{pmatrix} \\
 G_x &= \frac{1}{2h_x} \begin{pmatrix} 0 & 1 & & -1 \\ -1 & 0 & 1 & \\ & \ddots & \ddots & \ddots \\ & & 1 & 0 \\ 1 & & & -1 & 0 \end{pmatrix} \\
 G_x^T &= \frac{1}{2h_x} \begin{pmatrix} 0 & -1 & & 1 \\ 1 & 0 & -1 & \\ & \ddots & \ddots & \ddots \\ & & 1 & -1 \\ -1 & & & 1 & 0 \end{pmatrix}.
 \end{aligned}$$

Analyzing each term for the Fourier modes yields

$$\begin{aligned}
 (K_t \otimes M_x^1) u_h &\longrightarrow \frac{-U^{n-1} + 2U^n - U^{n+1}}{h_t} \frac{h_x}{6} (e^{i(m-1)\pi h_x} + 4e^{im\pi h_x} + e^{i(m+1)\pi h_x}) \\
 &= \frac{h_x}{6h_t} (-U^{n-1} + 2U^n - U^{n+1}) (2\cos(h_x\pi) + 4) e^{im\pi h_x} \\
 (M_t^{0,1} \otimes G_x^T) \vec{p}_h &\longrightarrow -\frac{h_t}{2} (P^n + P^{n-1}) (e^{i\pi h_x} - e^{-i\pi h_x}) e^{im\pi h_x} \\
 &= -ih_t (P^n + P^{n-1}) \sin(h_x\pi) e^{im\pi h_x} \\
 (M_t^{1,0} \otimes G_x) \vec{u}_h &\longrightarrow ih_t (U^n + U^{n-1}) \sin(h_x\pi) e^{im\pi h_x} \\
 (M_t^0 \otimes M_x^1) \vec{p}_h &\longrightarrow \frac{1}{h_t} P^n (2\cos(h_x\pi) + 4) e^{im\pi h_x}.
 \end{aligned}$$

Solving (4.7) for P^n

$$P^n = -ih_t^2 \frac{\sin(h_x\pi)}{2\cos(h_x\pi) + 4} (U^n + U^{n+1})$$

and substituting into (4.6) results in

$$(\gamma + 1)U^{n+1} + 2(\gamma - 1)U^n + (\gamma + 1)U^{n-1} = 0,$$

where

$$\gamma = \frac{3h_t^4 \sin^2(h_x\pi)}{h_x (2\cos(h_x\pi) + 4)^2} > 0.$$

This is a two-step method with the characteristic polynomial

$$\rho(z) = (\gamma + 1)z^2 + 2(\gamma - 1)z + (\gamma + 1)$$

and its simple complex roots are given by

$$z_{1,2} = \frac{1 - \gamma \pm i\sqrt{4\gamma}}{1 + \gamma}.$$

For their absolute value it holds

$$|z_{1,2}| = \frac{(1 - \gamma)^2 + 4\gamma}{(1 + \gamma)^2} = \frac{\gamma^2 - 2\gamma + 1 + 4\gamma}{(1 + \gamma)^2} = \frac{(1 + \gamma)^2}{(1 + \gamma)^2} = 1,$$

so the root condition (Theorem 1.3) is fulfilled independent of h_t and h_x and hence the system is unconditionally stable. \square

4.3 Numerical Experiments

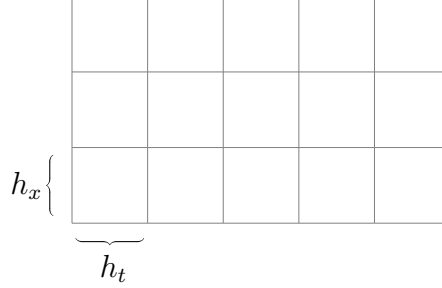


Figure 4.1: Quadrilateral Mesh

To verify the results of the previous sections, numerical computations are performed for different ratios $\frac{h_t}{h_x}$ on a regular quadrilateral mesh for $Q = (0, T) \times (0, 1)$. For the correct ordering of indices the degrees of freedom of this mesh can be identified with basis functions in the tensor product spaces. A sketch of a typical quadrilateral mesh is depicted in Figure 4.1. The known solution u for the numerical experiments is analogous to [14]

$$u(t, x) = t^2 \sin(\pi x),$$

which obviously fulfils the conditions on the initial and boundary data of the original variational problem (2.2). The convergence tables are done using an initial quadrilateral mesh with $h_x = \frac{1}{5}$ and h_t chosen according to the desired $\frac{h_t}{h_x}$ ratio, and subsequent uniform refinement. The final time T is chosen in a way that the desired ratio can be exactly achieved on the coarsest mesh for 20 time steps, i.e.

$$T = 20h_t.$$

4.3.1 Notes on Implementation

In this section quick notes on the implementation for tensor product spaces are given. Since dealing with different ansatz and test spaces is inconvenient (and in the case of irregular grids not always possible) the Galerkin-Bubnov variational formulation of the wave equation (2.3) is used. Even though some statements hold for more general settings, it is useful to limit the discussion to

$$\begin{aligned} X_h &= P^1(\mathcal{X}_h) \cap H_0^1(0, 1) \\ T_{h;0} &= P^1(\mathcal{T}_h) \cap H_0^1(0, T). \end{aligned}$$

Taking advantage of the fact that $U_h = T_{h,0} \otimes X_h$ the solution u_h has the representation (as in Remark 4.1)

$$u_h(t, x) = \sum_{i=1}^{\dim T_{h,0}} \sum_{k=1}^{\dim X_h} u_{i,k} \psi_i(t) \varphi_k(x) \quad u_{i,k} \in \mathbb{R},$$

where ψ_i are the nodal basis functions in time and φ_k in space. Replacing u_h in (2.3) by this representation and using Corollary 2.3 yield

$$\begin{aligned} \sum_{i=1}^{\dim T_{h,0}} \sum_{k=1}^{\dim X_h} u_{i,k} \left[\underbrace{\langle \partial_t \psi_i, \partial_t \psi_n \rangle_{L^2(0,T)}}_{K_t[n,i]} \underbrace{\langle \varphi_k, \varphi_r \rangle_{L^2(0,1)}}_{=M_x[r,k]} + \right. \\ \left. \underbrace{\langle \psi_i, T_R \psi_n \rangle_{L^2(0,T)}}_{=M_t^R[n,i]} \underbrace{\langle \partial_x \varphi_k, \partial_x \varphi_r \rangle_{L^2(0,1)}}_{=K_x[r,k]} \right] = \underbrace{\langle f, (T_R \psi_n) \varphi_r \rangle_{L^2(Q)}}_{=f_{n,r}^R}. \end{aligned}$$

$\forall \psi_n \in T_{h,0}, \forall \varphi_r \in X_h.$

With appropriate ordering of indices this corresponds to the system

$$(K_t \otimes M_x + M_t^R \otimes K_x) \vec{u} = \vec{f}^R,$$

where K_t, K_x are the standard temporal and spatial stiffness matrices and M_x is the standard spatial mass matrix. The mass matrix and the right hand side involving the modified time-reversal map are non standard. First consider the Matrix

$$M_t^R[n, i] = \langle \psi_i, \psi_n(T) \rangle_{L^2(0,T)} - \underbrace{\langle \psi_i, \psi_n \rangle_{L^2(0,T)}}_{M_t[n,i]},$$

where M_t is the standard temporal mass matrix and the first term can be calculated easily in most settings.

Remark 4.5. For $T_{h,0} = P^1(\mathcal{T}_h) \cap H_0^1(0, T)$ using a nodal basis it holds

$$\langle \psi_i, \psi_n(T) \rangle_{L^2(0,T)} = \begin{cases} \langle \psi_i, 1 \rangle_{L^2(0,T)} & \text{for } n = n_T \\ 0 & \text{else} \end{cases},$$

where n_T is the index of the degree of freedom at the node with $t_{n_T} = T$.

The right hand side is more difficult to evaluate

$$f_{n,r}^R = \langle f, (T_R \psi_n) \varphi_r \rangle_{L^2(Q)} = \langle f, \psi_n(T) \varphi_r \rangle_{L^2(Q)} - \underbrace{\langle f, \psi_n \varphi_r \rangle_{L^2(Q)}}_{f_{n,r}}.$$

$f_{n,r}$ is the standard load vector in the tensor product setting, but the term $\langle f, \psi_n(T) \varphi_r \rangle_{L^2(Q)}$ for e.g. piecewise linear ansatz functions in space and time, loses its locality in time

due to fixing $t = T$. This means that for the ansatz functions, where $\psi_n(T) \neq 0$ the integral

$$\langle f, \psi_n(T)\varphi_r \rangle_{L^2(Q)} = \psi_n(T) \int_0^T \int_{\text{supp}\varphi_r} f(t, x) \varphi_r(x) dt dx$$

has to be evaluated.

Remark 4.6. A convenient, yet computationally expensive way to calculate the integral, is to use the partition of unity in $P^1(\mathcal{T}_h)$

$$1 \equiv \sum_{i=1}^{\dim P^1(\mathcal{T}_h)} \psi_i,$$

where ψ_i are the nodal basis functions of $P^1(\mathcal{T}_h)$. Note that these are the same functions as in the representation of u_h with only one index more, due to non-existent boundary conditions in $P^1(\mathcal{T}_h)$. Then

$$\begin{aligned} \int_0^T \int_{\text{supp}\varphi_r} f(t, x) \varphi_r(x) dt dx &= \int_Q f(t, x) \varphi_r(x) dt dx = \int_Q 1 f(t, x) \varphi_r(x) dt dx = \\ &= \sum_{i=1}^{\dim P^1(\mathcal{T}_h)} \underbrace{\int_Q f(t, x) \psi_i(t) \varphi_r^x(x) dt dx}_{=f_{i,r}} = \sum_{i=1}^{\dim P^1(\mathcal{T}_h)} f_{i,r}, \end{aligned}$$

where the calculation of $f_{i,r}$ is usually a standard task in every finite element software.

Remark 4.7. If f can be written as a product

$$f(t, x) = f^t(t) f^x(x),$$

then

$$\langle f, \psi_n(T)\varphi_r \rangle_{L^2(Q)} = \psi_n(T) \langle f^t, 1 \rangle_{L^2(0,T)} \langle f^x, \varphi_r \rangle_{L^2(0,1)}$$

simplifying computations.

Remark 4.8. For structured grids the modified time-reversal map is an endomorphism, i.e.

$$T_R : P^1(\mathcal{T}_h) \longrightarrow P^1(\mathcal{T}_h).$$

This holds true since

$$T_R \varphi_i(t, x) = \varphi_i(T, x) - \varphi_i(t, x)$$

and $\varphi_i(T, x) \in P^1(\mathcal{T}_h)$ for structured quadrilateral and triangular grids. Hence the variational formulation (2.3) is equivalent to (2.2) even in the discrete setting and the Galerkin-Petrov formulation can be directly implemented.

The projections needed for the stabilizations are implemented by the reinterpretation as a system (4.1) and using the modified time reversal map, i.e. find $u_h \in U_h, p_h \in P_h$ such that

$$\begin{aligned} \langle \partial_t u_h, \partial_t v_h \rangle_{L^2(Q)} + \langle p_h, \partial_x T_R v_h \rangle_{L^2(Q)} &= \langle f, T_R v_h \rangle_Q \\ \langle \partial_x u_h, q_h \rangle_{L^2(Q)} - \langle p_h, q_h \rangle_{L^2(Q)} &= 0 \quad \forall v_h \in U_h, q_h \in P_h \end{aligned}$$

with appropriately chosen P_h (see the previous chapters).

4.3.2 Unstabilized Problem

In this section the unstabilized problem (2.3) is investigated for

$$U_h = (P^1(\mathcal{T}_h) \cap H_0^1(0, T)) \otimes (P^1(\mathcal{X}_h) \cap H_0^1(0, 1)).$$

For tensor product spaces the formulation is stable for

$$h_t \leq h_x$$

since in equation (4.4) $c_I = 1$ in this setting (see [14, page 192]). The numerical results in Tables 4.1 to 4.4 show that this condition is sharp and the expected convergence rates are observed.

Table 4.1: Numerical observations $\frac{h_t}{h_x} = 0.5$

Refinements	DOF	$\ u - u_h\ _{L^2(Q)}$	eoc	$ u - u_h _{H^1(Q)}$	eoc
0	126	0.054393	-	1.02022	-
1	451	0.0136738	1.99201	0.510399	0.999182
2	1701	0.00342315	1.99802	0.255231	0.999825
3	6601	0.000856116	1.99945	0.127619	0.999958
4	26001	0.000214068	1.99974	0.06381	0.99999
5	103201	5.35285e-05	1.99969	0.031905	0.999997

Table 4.2: Numerical observations $\frac{h_t}{h_x} = 1$

Refinements	DOF	$\ u - u_h\ _{L^2(Q)}$	eoc	$ u - u_h _{H^1(Q)}$	eoc
0	126	0.322253	-	5.75	-
1	451	0.0812576	1.98762	2.88196	0.996513
2	1701	0.020359	1.99684	1.44184	0.999138
3	6601	0.00509297	1.99909	0.721027	0.999785
4	26001	0.00127366	1.99953	0.360527	0.999946
5	103201	0.00031855	1.99939	0.180265	0.999986

Table 4.3: Numerical observations $\frac{h_t}{h_x} = 1.1$

Refinements	DOF	$\ u - u_h\ _{L^2(Q)}$	eoc	$ u - u_h _{H^1(Q)}$	eoc
0	126	0.410066	-	7.29574	-
1	451	0.103414	1.98743	3.65701	0.996389
2	1701	43.9328	-8.73073	3963.22	-10.0818
3	6601	57.3166	-0.383653	10316.2	-1.38017
4	26001	583.629	-3.34803	209153	-4.34158
5	103201	75.4169	2.95209	54250.8	1.94684

Table 4.4: Numerical observations $\frac{h_t}{h_x} = 3$

Refinements	DOF	$\ u - u_h\ _{L^2(Q)}$	eoc	$ u - u_h _{H^1(Q)}$	eoc
0	126	5.31797	-	91.1664	-
1	451	352985	-16.0184	1.00614e+07	-16.7519
2	1701	75618	2.22281	3.42636e+06	1.55408
3	6601	641868	-3.08548	6.54392e+07	-4.25541
4	26001	2710.23	7.88772	557638	6.87468
5	103201	12555.7	-2.21185	4.87947e+06	-3.12933

4.3.3 Projection onto Piecewise Constants in Time and Space

In this section the results of chapter 4.1, i.e.

$$p_h = Q_{h,t}^0 \partial_x u_h$$

are numerically verified. In Tables 4.5 to 4.8 the expected convergence behaviour can be observed independently of the $\frac{h_t}{h_x}$ ratio.

Table 4.5: Numerical observations $\frac{h_t}{h_x} = 0.5$

Refinements	DOF	$\ u - u_h\ _{L^2(Q)}$	eoc	$ u - u_h _{H^1(Q)}$	eoc
0	126	0.0551079	-	1.02001	-
1	451	0.0138823	1.98901	0.510372	0.998962
2	1701	0.00347757	1.99709	0.255227	0.999767
3	6601	0.000869871	1.99921	0.127619	0.999943
4	26001	0.000217516	1.99968	0.0638099	0.999986
5	103201	5.43912e-05	1.99968	0.031905	0.999996

Table 4.6: Numerical observations $\frac{h_t}{h_x} = 1$

Refinements	DOF	$\ u - u_h\ _{L^2(Q)}$	eoc	$ u - u_h _{H^1(Q)}$	eoc
0	126	0.328683	-	5.75021	-
1	451	0.0829207	1.98689	2.88198	0.996551
2	1701	0.02078	1.99654	1.44184	0.999148
3	6601	0.00519857	1.99901	0.721028	0.999788
4	26001	0.00130008	1.99951	0.360527	0.999947
5	103201	0.000325157	1.9994	0.180265	0.999987

Table 4.7: Numerical observations $\frac{h_t}{h_x} = 3$

Refinements	DOF	$\ u - u_h\ _{L^2(Q)}$	eoc	$ u - u_h _{H^1(Q)}$	eoc
0	126	5.22858	-	89.5611	-
1	451	1.32201	1.98369	44.9044	0.996016
2	1701	0.331054	1.99759	22.4674	0.999021
3	6601	0.0827321	2.00055	11.2356	0.999755
4	26001	0.0206908	1.99946	5.61805	0.999939
5	103201	0.00517835	1.99842	2.80905	0.999984

Table 4.8: Numerical observations $\frac{h_t}{h_x} = 8$

Refinements	DOF	$\ u - u_h\ _{L^2(Q)}$	eoc	$ u - u_h _{H^1(Q)}$	eoc
0	126	60.8766	-	1039.95	-
1	451	15.3442	1.9882	521.417	0.996001
2	1701	3.84253	1.99756	260.89	0.998998
3	6601	0.963279	1.99603	130.467	0.99975
4	26001	0.241428	1.99636	65.2365	0.999938
5	103201	0.0605098	1.99635	32.6186	0.999984

4.3.4 Projection onto Piecewise Constants in Time and Piecewise Linears in Space

In this section the results of chapter 4.2, i.e.

$$p_h = (Q_{t,x}^0 \otimes Q_{h,x}^1) \partial_x u_h$$

are numerically verified. In Tables 4.5 to 4.8 the expected convergence behaviour can be observed independently of the $\frac{h_t}{h_x}$ ratio.

Table 4.9: Numerical observations $\frac{h_t}{h_x} = 0.5$

Refinements	DOF	$\ u - u_h\ _{L^2(Q)}$	eoc	$ u - u_h _{H^1(Q)}$	eoc
0	126	0.00820017	-	1.03355	-
1	451	0.00114303	2.84279	0.511878	1.01373
2	1701	0.00021055	2.44063	0.25541	1.00299
3	6601	4.70813e-05	2.16094	0.127641	1.00072
4	26001	1.14016e-05	2.04592	0.0638128	1.00018
5	103201	2.82695e-06	2.01191	0.0319054	1.00004

Table 4.10: Numerical observations $\frac{h_t}{h_x} = 1$

Refinements	DOF	$\ u - u_h\ _{L^2(Q)}$	eoc	$ u - u_h _{H^1(Q)}$	eoc
0	126	0.0449745	-	5.83837	-
1	451	0.00631931	2.83127	2.89204	1.01348
2	1701	0.00117895	2.42227	1.44307	1.00294
3	6601	0.000265495	2.15074	0.72118	1.00071
4	26001	6.44434e-05	2.04258	0.360546	1.00018
5	103201	1.59883e-05	2.01101	0.180268	1.00004

Table 4.11: Numerical observations $\frac{h_t}{h_x} = 3$

Refinements	DOF	$\ u - u_h\ _{L^2(Q)}$	eoc	$ u - u_h _{H^1(Q)}$	eoc
0	126	0.694725	-	90.9766	-
1	451	0.0967634	2.84391	45.0651	1.01349
2	1701	0.0182339	2.40784	22.4871	1.00291
3	6601	0.00412936	2.14263	11.2381	1.0007
4	26001	0.00100401	2.04014	5.61835	1.00018
5	103201	0.000249203	2.01038	2.80909	1.00004

Table 4.12: Numerical observations $\frac{h_t}{h_x} = 8$

Refinements	DOF	$\ u - u_h\ _{L^2(Q)}$	eoc	$ u - u_h _{H^1(Q)}$	eoc
0	126	8.14022	-	1056.48	-
1	451	1.08172	2.91174	523.303	1.01355
2	1701	0.20194	2.42133	261.121	1.00293
3	6601	0.0471514	2.09855	130.496	1.00071
4	26001	0.0116381	2.01844	65.2401	1.00018
5	103201	0.00289232	2.00856	32.619	1.00004

5 Regular Triangular Meshes

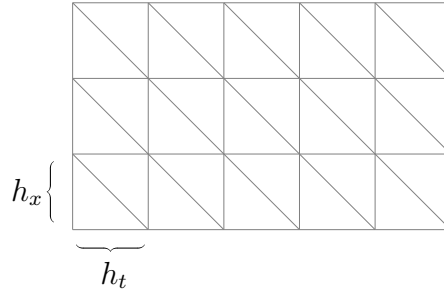


Figure 5.1: Triangular Mesh

This chapter tries to transfer the results for tensor product spaces to regular triangular meshes as depicted in Figure 5.1, but it was not possible for the author to find a unconditionally stable formulation. The main reason for this is the inherent coupling of space and time on triangular meshes, which aggravates the analysis and implementation. The onset for all considered stabilizations is the reinterpretation of the variational problem (4.1) with different function spaces, i.e. to find $u_h \in U_h, p_h \in P_h$ such that

$$\begin{aligned} \langle \partial_t u_h, \partial_t v_h \rangle_{L^2(Q)} + \langle p_h, \partial_x T_R v_h \rangle_{L^2(Q)} &= \langle f, T_R v_h \rangle_Q \\ - \langle \partial_x u_h, q_h \rangle_{L^2(Q)} + \langle p_h, q_h \rangle_{L^2(Q)} &= 0 \quad \forall v_h \in U_h, q_h \in P_h, \end{aligned}$$

where u_h is chosen to be piecewise linear. For this purpose let \mathcal{Q}_h be a decomposition of Q into triangles, as depicted in Figure 5.1. Then

$$U_h = P^1(\mathcal{Q}_h) \cap H_{0;0}^{1,1}(Q).$$

The space P_h is chosen dependent on the desired stabilization. Three different cases are considered

- $P_h = P^0(\mathcal{Q}_h)$ (no stabilization)
- $P_h = P^1(\mathcal{Q}_h) \cap H^1(Q)$
- $P_h = P^1(\mathcal{Q}_h) \cap H^1(Q)$ with mass lumping

Due to the problems in proving the theory and since the goal of finding a unconditionally stable formulation is not met, only numerical experiments are presented. The variational problem in matrix form reads as

$$\begin{pmatrix} K & G^R \\ -G & M \end{pmatrix} \begin{pmatrix} \vec{u}_h \\ \vec{p}_h \end{pmatrix} = \begin{pmatrix} \vec{f}^R \\ 0 \end{pmatrix} \quad (5.1)$$

where the matrices and vectors are associated in the following way:

$$\begin{aligned} K &\longleftrightarrow \langle \partial_t u_h, \partial_t v_h \rangle_{L^2(Q)} = -\langle \partial_t u_h, \partial_t T_R v_h \rangle_{L^2(Q)} \\ G^R &\longleftrightarrow \langle p_h, \partial_x T_R v_h \rangle_{L^2(Q)} \\ G &\longleftrightarrow \langle \partial_x u_h, q_h \rangle_{L^2(Q)} \\ M &\longleftrightarrow \langle p_h, q_h \rangle_{L^2(Q)} \\ \vec{f}^R &\longleftrightarrow \langle f, T_R v_h \rangle_{L^2(Q)}. \end{aligned}$$

5.1 Numerical Experiments

The setup is the same as in chapter 4.3 only for triangular meshes.

5.1.1 No Stabilization

If no stabilization is applied, i.e. $P_h = P^0(Q_h)$ ($\partial_x u_h$ is already in P_h in that case). A similar CLF-condition

$$h_t \leq h_x$$

is observed, as the results in Tables 5.1 to 5.4 indicate.

Table 5.1: Numerical observations $\frac{h_t}{h_x} = 0.5$

Refinements	DOF	$\ u - u_h\ _{L^2(Q)}$	eoc	$ u - u_h _{H^1(Q)}$	eoc
0	126	0.0634581	-	1.21118	-
1	451	0.0159852	1.98907	0.607763	0.994831
2	1701	0.00400397	1.99724	0.304152	0.998717
3	6601	0.00100151	1.99926	0.15211	0.99968
4	26001	0.000250426	1.99972	0.076059	0.99992
5	103201	6.26181e-05	1.99973	0.0380301	0.99998

Table 5.2: Numerical observations $\frac{h_t}{h_x} = 1$

Refinements	DOF	$\ u - u_h\ _{L^2(Q)}$	eoc	$ u - u_h _{H^1(Q)}$	eoc
0	126	0.340945	-	6.20446	-
1	451	0.085991	1.98728	3.11415	0.994467
2	1701	0.0215461	1.99676	1.55856	0.998626
3	6601	0.00538997	1.99908	0.779464	0.999657
4	26001	0.00134791	1.99955	0.389755	0.999914
5	103201	0.000337107	1.99945	0.19488	0.999978

Table 5.3: Numerical observations $\frac{h_t}{h_x} = 1.1$

Refinements	DOF	$\ u - u_h\ _{L^2(Q)}$	eoc	$ u - u_h _{H^1(Q)}$	eoc
0	126	18.1175	-	402.344	-
1	451	139671	-12.9124	6.19829e+06	-13.9112
2	1701	4.01968e+08	-11.4908	3.60724e+10	-12.5067
3	6601	8.48984e+06	5.5652	1.52596e+09	4.56311
4	26001	1.2915e+07	-0.605235	4.62869e+09	-1.60089
5	103201	159820	6.33645	1.14563e+08	5.33639

Table 5.4: Numerical observations $\frac{h_t}{h_x} = 3$

Refinements	DOF	$\ u - u_h\ _{L^2(Q)}$	eoc	$ u - u_h _{H^1(Q)}$	eoc
0	126	1.21493e+14	-	1.74532e+15	-
1	451	3.89135e+12	4.96445	1.1236e+14	3.95729
2	1701	2.71362e+11	3.84198	1.54127e+13	2.86595
3	6601	8.03062e+10	1.75663	8.87667e+12	0.796025
4	26001	2.05512e+09	5.28821	4.67112e+11	4.24818
5	103201	2.19981e+09	-0.0981525	8.84974e+11	-0.921866

5.1.2 Projection onto Piecewise Linears

In this section the projection of $\partial_x u_h$ onto piecewise linears is considered, i.e. $P_h = P^1(\mathcal{Q}_h) \cap H^1(Q)$. Here an approximate CLF-condition

$$h_t < 4h_x$$

is observed numerically as Tables 5.5 to 5.10 indicate.

Table 5.5: Numerical observations $\frac{h_t}{h_x} = 0.5$

Refinements	DOF	$\ u - u_h\ _{L^2(Q)}$	eoc	$ u - u_h _{H^1(Q)}$	eoc	$\ p - p_h\ _{L^2(Q)}$	eoc
0	126	0.026263	-	1.24981	-	0.0850616	-
1	451	0.00581525	2.17512	0.612712	1.02843	0.0242824	1.8086
2	1701	0.0014324	2.02141	0.305558	1.00376	0.00615973	1.97897
3	6601	0.000356805	2.00522	0.152682	1.00092	0.00161582	1.9306
4	26001	8.91285e-05	2.00118	0.076329	1.00022	0.000441076	1.87317
5	103201	2.22805e-05	2.00011	0.0381631	1.00005	0.000126802	1.79845

Table 5.6: Numerical observations $\frac{h_t}{h_x} = 1$

Refinements	DOF	$\ u - u_h\ _{L^2(Q)}$	eoc	$ u - u_h _{H^1(Q)}$	eoc	$\ p - p_h\ _{L^2(Q)}$	eoc
0	126	0.112785	-	6.40532	-	0.350524	-
1	451	0.0231841	2.28237	3.14068	1.02819	0.111721	1.64961
2	1701	0.00563654	2.04025	1.56668	1.00336	0.0290181	1.94488
3	6601	0.00139977	2.00962	0.782908	1.0008	0.00792617	1.87226
4	26001	0.00034952	2.00174	0.391408	1.00017	0.00221978	1.8362
5	103201	8.74145e-05	1.99943	0.195704	0.999999	0.000636252	1.80275

Table 5.7: Numerical observations $\frac{h_t}{h_x} = 3.8$

Refinements	DOF	$\ u - u_h\ _{L^2(Q)}$	eoc	$ u - u_h _{H^1(Q)}$	eoc	$\ p - p_h\ _{L^2(Q)}$	eoc
0	126	3.309	-	174.51	-	11.5793	-
1	451	0.664393	2.31629	85.6063	1.02752	3.71786	1.639
2	1701	0.158049	2.07166	42.6794	1.00418	1.12409	1.72571
3	6601	0.0402786	1.97229	21.3589	0.998704	0.538694	1.06122
4	26001	0.00966136	2.05972	10.6563	1.00313	0.162774	1.7266
5	103201	0.00250317	1.94847	5.33781	0.997384	0.121863	0.41761

Table 5.8: Numerical observations $\frac{h_t}{h_x} = 4$

Refinements	DOF	$\ u - u_h\ _{L^2(Q)}$	eoc	$ u - u_h _{H^1(Q)}$	eoc	$\ p - p_h\ _{L^2(Q)}$	eoc
0	126	5.70281	-	207.372	-	25.2597	-
1	451	1.00907	2.49865	99.3723	1.06131	7.16957	1.81688
2	1701	0.281389	1.84239	50.1695	0.986033	3.82657	0.905834
3	6601	0.0650491	2.11296	24.8184	1.0154	1.70981	1.16222
4	26001	0.0235376	1.46656	12.807	0.954482	1.41674	0.271257
5	103201	0.00792454	1.57057	6.55317	0.966665	1.03326	0.455372

Table 5.9: Numerical observations $\frac{h_t}{h_x} = 4.2$

Refinements	DOF	$\ u - u_h\ _{L^2(Q)}$	eoc	$ u - u_h _{H^1(Q)}$	eoc	$\ p - p_h\ _{L^2(Q)}$	eoc
0	126	12.9769	-	287.67	-	60.3472	-
1	451	0.988391	3.71472	110.763	1.37694	6.3491	3.24866
2	1701	0.455472	1.11772	59.3829	0.899355	6.48477	-0.0305031
3	6601	0.520153	-0.191573	66.2935	-0.158819	14.1065	-1.12123
4	26001	0.281037	0.888178	72.1511	-0.122154	14.2477	-0.0143771
5	103201	0.299769	-0.0930927	157.53	-1.12653	29.7805	-1.06364

Table 5.10: Numerical observations $\frac{h_t}{h_x} = 8$

Refinements	DOF	$\ u - u_h\ _{L^2(Q)}$	eoc	$ u - u_h _{H^1(Q)}$	eoc	$\ p - p_h\ _{L^2(Q)}$	eoc
0	126	61143.3	-	594178	-	232793	-
1	451	6.10142e+10	-19.9285	1.31259e+12	-21.075	4.63941e+11	-20.9265
2	1701	7.50884e+12	-6.9433	2.97489e+14	-7.82428	1.2548e+14	-8.0793
3	6601	1.20762e+11	5.95836	9.67575e+12	4.94232	3.87466e+12	5.01724
4	26001	7.11199e+10	0.763838	1.3663e+13	-0.497834	4.51474e+12	-0.220571
5	103201	1.61206e+14	-11.1464	5.35108e+16	-11.9353	1.91065e+16	-12.0471

5.1.3 Projection onto Piecewise Linears with Mass Lumping

In this section the projection of $\partial_x u_h$ onto piecewise linears is considered, i.e. $P_h = P^1(Q_h)$, but in this case the matrix M in (5.1) is replaced with its lumped mass matrix \tilde{M}

$$\tilde{M}[i, j] = \delta_{i,j} \sum_{j=1}^{\dim P_h} M[i, j].$$

This approach is inspired by [3], where a pressure stabilization for the similar Stokes problem is introduced. This approach is especially interesting, since the lumped mass matrix can be easily inverted and hence p can be efficiently eliminated. This approach greatly improves stability, however an approximate CFL-condition

$$h_t < 7.5h_x$$

is observed numerically as Tables 5.11 to 5.15 indicate.

Table 5.11: Numerical observations $\frac{h_t}{h_x} = 0.5$

Refinements	DOF	$\ u - u_h\ _{L^2(Q)}$	eoc	$ u - u_h _{H^1(Q)}$	eoc	$\ p - p_h\ _{L^2(Q)}$	eoc
0	126	0.109003	-	1.44374	-	0.221464	-
1	451	0.0267963	2.02427	0.63754	1.17922	0.0703795	1.65385
2	1701	0.00668162	2.00376	0.31113	1.035	0.0235317	1.58055
3	6601	0.00166906	2.00116	0.15461	1.00888	0.00810296	1.53808
4	26001	0.000417159	2.00037	0.077186	1.00222	0.00282759	1.51887
5	103201	0.000104274	2.00021	0.0385782	1.00055	0.000993272	1.50931

Table 5.12: Numerical observations $\frac{h_t}{h_x} = 1$

Refinements	DOF	$\ u - u_h\ _{L^2(Q)}$	eoc	$ u - u_h _{H^1(Q)}$	eoc	$\ p - p_h\ _{L^2(Q)}$	eoc
0	126	0.674373	-	7.45317	-	1.0536	-
1	451	0.161841	2.05897	3.28055	1.18392	0.36294	1.53753
2	1701	0.0402232	2.00848	1.59901	1.03676	0.127314	1.51134
3	6601	0.0100394	2.00235	0.794383	1.00927	0.0448246	1.50602
4	26001	0.00250861	2.00071	0.396565	1.00228	0.0158186	1.50267
5	103201	0.000626969	2.00042	0.198207	1.00055	0.00558832	1.50113

Table 5.13: Numerical observations $\frac{h_t}{h_x} = 7.5$

Refinements	DOF	$\ u - u_h\ _{L^2(Q)}$	eoc	$ u - u_h _{H^1(Q)}$	eoc	$\ p - p_h\ _{L^2(Q)}$	eoc
0	126	127.77	-	1471.22	-	181.348	-
1	451	26.6757	2.25995	496.324	1.56766	51.2307	1.82368
2	1701	6.56254	2.0232	244.079	1.02393	19.0163	1.42977
3	6601	1.6539	1.98838	126.736	0.945521	7.86861	1.27306
4	26001	0.454697	1.8629	71.9159	0.817447	5.24161	0.586098
5	103201	0.108761	2.06374	33.248	1.11304	2.04188	1.36011

Table 5.14: Numerical observations $\frac{h_t}{h_x} = 7.6$

Refinements	DOF	$\ u - u_h\ _{L^2(Q)}$	eoc	$ u - u_h _{H^1(Q)}$	eoc	$\ p - p_h\ _{L^2(Q)}$	eoc
0	126	136.547	-	1612.06	-	195.77	-
1	451	27.7773	2.29741	524.886	1.61883	53.8799	1.86134
2	1701	7.07907	1.97227	281.447	0.899144	22.215	1.27821
3	6601	1.90484	1.89389	156.847	0.843508	12.0782	0.879134
4	26001	0.430275	2.14634	66.0645	1.24741	3.51615	1.78033
5	103201	0.167444	1.36158	49.1855	0.425642	5.63027	-0.679207

Table 5.15: Numerical observations $\frac{h_t}{h_x} = 8$

Refinements	DOF	$\ u - u_h\ _{L^2(Q)}$	eoc	$ u - u_h _{H^1(Q)}$	eoc	$\ p - p_h\ _{L^2(Q)}$	eoc
0	126	180.372	-	2321.64	-	266.591	-
1	451	35.9232	2.32799	797.009	1.54248	81.9693	1.70148
2	1701	11.6889	1.61977	525.308	0.601432	50.2763	0.705205
3	6601	34146.8	-11.5124	2.96521e+06	-12.4627	334700	-12.7007
4	26001	2.21185e+09	-15.9831	4.03947e+11	-17.0557	4.18818e+10	-16.9331
5	103201	1.79621e+07	6.94415	5.99328e+09	6.07468	7.18787e+08	5.86461

6 Conclusion and Outlook

In this work finite element methods for the wave equation in space-time and possible stabilization techniques are explored. For tensor product ansatz spaces previous work is revisited and a new unconditionally stable formulation is found. On structured triangular grids the restrictions on the meshes could be substantially relaxed, but unfortunately this is not directly transferable to unstructured grids.

There is ongoing work in the research group at the Institute for Applied Mathematics at Graz, University of Technology, investigating the use of the modified Hilbert transform introduced in [14] instead of the modified time-reversal map. For this approach there are promising numerical results, but the proofs and an efficient implementation on unstructured grids are still missing.

Further research with promising results is done in the same group taking ideas from optimal control. However this approach is still very new and needs further investigation.

Bibliography

- [1] W. Arendt and K. Urban. *Partielle Differenzialgleichungen: Eine Einführung in analytische und numerische Methoden*. Springer Berlin Heidelberg, 2018. ISBN: 978-3-662-58322-7.
- [2] S. Bartels. *Numerical approximation of partial differential equations*. Vol. 64. Texts in Applied Mathematics. Springer, 2016. ISBN: 978-3-319-32353-4; 978-3-319-32354-1.
- [3] R. Becker and P. Hansbo. “A simple pressure stabilization method for the Stokes equation”. In: *Comm. Numer. Methods Engrg.* 24.11 (2008). ISSN: 1069-8299.
- [4] J. Ernesti and C. Wieners. “Space-time discontinuous Petrov-Galerkin methods for linear wave equations in heterogeneous media”. In: *Comput. Methods Appl. Math.* 19.3 (2019). ISSN: 1609-4840.
- [5] W. Gautschi. *Numerical analysis*. Birkhäuser Boston, Inc., Boston, MA, 2012. ISBN: 978-0-8176-8258-3.
- [6] J. Gopalakrishnan and P. Sepúlveda. “A space-time DPG method for the wave equation in multiple dimensions”. In: *Space-time methods—applications to partial differential equations*. Vol. 25. Radon Ser. Comput. Appl. Math. De Gruyter, Berlin, 2019.
- [7] E. Hairer and G. Wanner. *Solving ordinary differential equations. II*. Vol. 14. Springer Series in Computational Mathematics. Springer-Verlag, Berlin, 2010. ISBN: 978-3-642-05220-0.
- [8] E. Isaacson and H. B. Keller. *Analysis of numerical methods*. Dover Publications, Inc., New York, 1994. ISBN: 0-486-68029-0.
- [9] M. Kreuter. “Sobolev Spaces of Vector-Valued Functions”. MA thesis. Ulm University, Faculty of Mathematics and Economics, 2015.
- [10] *MFEM: Modular Finite Element Methods [Software]*. mfem.org.
- [11] O. Steinbach. *Numerical Approximation Methods for Elliptic Boundary Value Problems: Finite and Boundary Elements*. Springer New York, 2008.
- [12] O. Steinbach and M. Zank. “A generalized inf-sup stable variational formulation for the wave equation”. In: *J. Math. Anal. Appl.* 505.1 (2022). ISSN: 0022-247X.

- [13] O. Steinbach and M. Zank. “A stabilized space-time finite element method for the wave equation”. In: *Advanced finite element methods with applications*. Vol. 128. Lect. Notes Comput. Sci. Eng. Springer, Cham, 2019.
- [14] O. Steinbach and M. Zank. “Coercive space-time finite element methods for initial boundary value problems”. In: *Electron. Trans. Numer. Anal.* 52 (2020).
- [15] E. Süli and D. F. Mayers. *An introduction to numerical analysis*. Cambridge University Press, Cambridge, 2003. ISBN: 0-521-81026-4; 0-521-00794-1.
- [16] U. Trottenberg, C. W. Oosterlee, and A. Schüller. *Multigrid*. Academic Press, Inc., San Diego, CA, 2001. ISBN: 0-12-701070-X.
- [17] M. Zank. *Inf-sup stable space-time methods for time-dependent partial differential equations*. Verlag der Technischen Universität Graz, 2020.
- [18] A. A. Zlotnik. “Convergence rate estimates of finite-element methods for second-order hyperbolic equations”. In: *Numerical methods and applications*. CRC, Boca Raton, FL, 1994.

AFFIDAVIT

I declare that I have authored this thesis independently, that I have not used other than the declared sources/resources, and that I have explicitly indicated all material which has been quoted either literally or by content from the sources used. The text document uploaded to TUGRAZonline is identical to the present master's thesis.

Date

Signature